

Elsevier Editorial System(tm) for Quaternary International
Manuscript Draft

Manuscript Number: QUATINT-D-12-00191R1

Title: Multiproxy evidence for abrupt climate change impacts on terrestrial and freshwater ecosystems in the Ol'khon region of Lake Baikal, central Asia

Article Type: Baikal-Hokkaido

Keywords: climate reconstruction; pollen; ostracod; geochemistry; shallow lake, central Asia

Corresponding Author: Dr Anson W. Mackay, Ph.D.

Corresponding Author's Institution: UCL

First Author: Anson Mackay

Order of Authors: Anson Mackay; Elena Bezrukova; John Boyle; Jonathan Holmes; Virginia Panizzo; Natalia Piotrowska; Alexander Shchetnikov; Ewan Shilland; Pavel Tarasov; Dustin White

Manuscript Region of Origin: RUSSIAN FEDERATION

Abstract: A palaeolimnological study of Lake Khall was undertaken to reconstruct impacts from five thousand years of climate change and human activity in the Ol'khon region of Lake Baikal. Taiga biome dominated regional landscapes, although significant compositional turnover occurred due to the expansion of eurythermic and drought resistant Scots pine. Climate during the mid-Holocene was wetter than the present, and Lake Khall was fresh, with abundant molluscs. By 4.4 cal ka BP, sedimentary geochemistry indicated a gradual change in lake water chemistry with an increase in lake salinity up to the present day, most likely controlled by groundwater influences. Vegetation turnover rate was highest between 2.75 - 2.48 cal ka BP, with the onset of drier, more continental climate, which resulted in an influx of aeolian particles to the lake. This abrupt shift was coincident with ice rafted debris event (IRD-2) in North Atlantic sediments and an attenuation of the East Asian summer monsoon. A second arid period occurred shortly afterwards (2.12 - 1.87 cal ka BP) which resulted in the decline in ostracod numbers, especially *Candona* sp. A rather more quiescent, warmer period followed, between 1.9 - 0.7 cal ka BP, with very little change in vegetation composition, and low amounts of detrital transfer from catchment to the lake. Peak reconstructed temperatures (and low amounts of annual precipitation) were concurrent with the Medieval Climate Anomaly. Between 0.77 - 0.45 cal ka BP, climate in the Ol'khon region became colder and wetter, although Lake Khall did not become more fresh. Cold, wet conditions are seen at other sites around Lake Baikal, and therefore represent a regional response to the period concurrent with the Little Ice Age and IRD-0. After AD 1845 the region warms, and *Pediastrum* appears in the lake in high abundances for the first time. We ascribe this increase to nutrient enrichment in the lake, linked to the rapid increase in regional pastoral farming.

1 Multiproxy evidence for abrupt climate change impacts on terrestrial and freshwater
2 ecosystems in the Ol'khon region of Lake Baikal, central Asia.

3

4 Anson W. Mackay^{a,*}, Elena V. Bezrukova^b, John F. Boyle^c, Jonathan A. Holmes^a, Virginia N.
5 Panizzo^a, Natalia Piotrowska^d, Alexander Shchetnikov^e, Ewan M. Shilland^a, Pavel Tarasov^f,
6 Dustin White^g

7

8 * Corresponding author: *Email address:* a.mackay@ucl.ac.uk

9 Phone : +44 (0)20 7679 0558 ; Fax : +44 (0)20 7679 0565

10

11 ^a*Environmental Change Research Centre, Department of Geography, UCL, Gower Street,*
12 *London, WC1E 6BT, UK.*

13 Email: a.mackay@ucl.ac.uk

14

15 ^b*Institute of Geochemistry, Russian Academy of Sciences, Siberian Branch, Irkutsk, Russia.*

16 Email: bezrukova@igc.irk.ru

17

18 ^c*Department of Geography, The University of Liverpool, Roxby Building, Liverpool L69 7ZT,*
19 *UK.*

20 Email: jfb@liverpool.ac.uk

21

22 ^d*Institute of Physics, Department of Radioisotopes, GADAM Centre of Excellence, Silesian*
23 *University of Technology, Krzywoustego 2, 44-100 Gliwice, Poland.*

24 Email: natalia.piotrowska@polsl.pl

25

26 ^e*Institute of Earth's Crust, Russian Academy of Sciences, Siberian Branch, Irkutsk, Russia.*

27 Email: shchet@crust.irk.ru

28

29 ^f*Institute of Geological Sciences, Palaeontology, Freie University Berlin, Malteserstrasse 74-*
30 *100, Building D, 12249 Berlin, Germany.*

31 Email: ptarasov@zedat.fu-berlin.de

32

33 ^g*Archaeology, University of Southampton, Avenue Campus, Southampton, SO17 1BF, UK.*

34 Email: dustin.white@soton.ac.uk

35

36

37

38

39 **Abstract**

40

41 A palaeolimnological study of Lake Khall was undertaken to reconstruct impacts from five
42 thousand years of climate change and human activity in the Ol'khon region of Lake Baikal.
43 Taiga biome dominated regional landscapes, although significant compositional turnover
44 occurred due to the expansion of eurythermic and drought resistant Scots pine. Climate during
45 the mid-Holocene was wetter than the present, and Lake Khall was fresh, with abundant
46 molluscs. By 4.4 cal ka BP, sedimentary geochemistry indicated a gradual change in lake
47 water chemistry with an increase in lake salinity up to the present day, most likely controlled
48 by groundwater influences. Vegetation turnover rate was highest between 2.75 – 2.48 cal ka
49 BP, with the onset of drier, more continental climate, which resulted in an influx of aeolian
50 particles to the lake. This abrupt shift was coincident with ice rafted debris event (IRD-2) in
51 North Atlantic sediments and an attenuation of the East Asian summer monsoon. A second
52 arid period occurred shortly afterwards (2.12 – 1.87 cal ka BP) which resulted in the decline
53 in ostracod numbers, especially *Candona* sp. A rather more quiescent, warmer period
54 followed, between 1.9 – 0.7 cal ka BP, with very little change in vegetation composition, and
55 low amounts of detrital transfer from catchment to the lake. Peak reconstructed temperatures
56 (and low amounts of annual precipitation) were concurrent with the Medieval Climate
57 Anomaly. Between 0.77 – 0.45 cal ka BP, climate in the Ol'khon region became colder and
58 wetter, although Lake Khall did not become more fresh. Cold, wet conditions are seen at
59 other sites around Lake Baikal, and therefore represent a regional response to the period
60 concurrent with the Little Ice Age and IRD-0. After AD 1845 the region warms, and
61 *Pediastrum* appears in the lake in high abundances for the first time. We ascribe this increase
62 to nutrient enrichment in the lake, linked to the rapid increase in regional pastoral farming.

63

64

65

66

67

68 **Keywords:** climate reconstruction; pollen; ostracod; geochemistry; shallow lake, central Asia

69 **1. Introduction**

70

71 Since 2001 a major interdisciplinary programme (Baikal Archaeology Project) has sought
72 to characterise Holocene cultural dynamics among hunter-gatherer and pastoralist populations
73 in central Asia (Weber et al., 2010). Results from this on-going research have redefined our
74 understanding of hunter-gatherer adaptive strategies during the Neolithic–Bronze Age,
75 including aspects of culture, subsistence and diet, mobility patterns, genetic structure, and
76 social and political relations. Most of these new archaeological data have been derived from
77 numerous well-preserved formal cemetery contexts, which has allowed detailed analyses of
78 human skeletal remains. Focus has especially centred on a distinct biocultural discontinuity
79 during the late Neolithic – early Bronze Age (Weber et al., 2002), and more recently the
80 expansion of pastoralist populations (Nomokonova et al., 2010).

81 One of the oldest records of human occupation in this region (ca. 9 ka BP) was recorded at
82 the Sagan-Zaba cove, in the Ol’khon region (known as *Priol’khon’e* in the Russian
83 geographical literature) of Lake Baikal (Nomokonova et al., in review). The white marble
84 cliffs adjacent to the cove are world renown for their petroglyphs, dating as far back as 4 ka
85 BP. Since the late Holocene, pastoralists dominated the Ol’khon region, herding a range of
86 animals including cattle, sheep, goats and horses (Nomokonova et al., 2010). Subsistence
87 patterns at Sagan-Zaba were more diverse than neighbouring regions, possibly because of the
88 relatively harsh environment, such that, unusual for pastoralists, these populations also hunted
89 *nerpa*, Lake Baikal’s freshwater seal.

90 Despite the long history of prehistoric populations around Lake Baikal, there is very little
91 evidence to suggest that they had a significant impact on regional landscapes (Tarasov et al.
92 2007). However, the pollen source area of Lake Baikal is vast and indicative of very broad
93 regional-scale variability (Sugita 1994), such as biomes (Seppä and Bennett, 2003; Tarasov et
94 al., 2007). One would not necessarily expect therefore Lake Baikal sediments to record
95 impacts from regional prehistoric populations. Smaller lakes have smaller source areas
96 (Jacobson and Bradshaw, 1981), and therefore potentially offer a better possibility for
97 disentangling natural (e.g. climatic) from anthropogenic impacts. Around Lake Baikal,
98 smaller lakes are increasingly being investigated (e.g. Tarasov et al., 2009; Ptitsyn et al.,
99 2010; Mackay et al., 2012), although very few studies have looked at palaeoenvironmental
100 changes in the semi-arid region to the west of the lake (Sklyarov et al., 2010).

101 The principal aim of this study is to provide a detailed palaeolimnological record of
102 environmental change in the climatically sensitive Ol’khon region of Lake Baikal, where
103 there is a long, dynamic history of human occupation.

104

105 **2. Geology and regional climate**

106

107 The study area lies to the south of Ol’khon Island on the west coast of Lake Baikal
108 and is represented by Paleozoic Ol’khon metamorphic terrane (Sklyarova et al., 2002). The
109 flat-topped Ol’khon Island and Ol’khon region form part of the Middle Baikal inter-basinal
110 link. Small grabens and horsts shape the link’s surface and form linear en-echelon systems.
111 The grabens are confined to two types of recent faults in the process: northeast linear faults
112 inherited from the Early Paleozoic structures and north-northeast pull-apart structures related
113 to late left-lateral strike-slip dislocations of the Baikal rift formation. Numerous fresh and
114 salt-water lakes are associated with these faults (Sklyarova et al., 2002), with their long-term
115 existence being dependent on faults draining deep, groundwater horizons (Sklyarov et al.,
116 2010). The study site, Lake Khall, is located on marble and surrounded by two intrusions –
117 Birkhinsky in the north (gabbro, gabbro-norites, olivine gabbro) and Tsagan-Zabinsky in the
118 south (andesites, andesite-basalts and basalts). It is a shallow, isometric, freshwater
119 bicarbonate lake located in a structural low of one these northeast linear faults. Lake Khall is
120 probably fed from subaqueous groundwater, and so its chemical composition reflects the
121 chemistry of the feeder groundwater (Sklyarova et al., 2002). The region is arid to semi-arid
122 because it sits in the rain shadow of the neighbouring Primorsky Mountain Range (Fig. 1).
123 Annual precipitation is low between 200 – 350 mm/yr (Atlas Baikala, 1993). Vegetation is

124 therefore a mixture between light coniferous taiga forest with fragmented steppe landscape,
125 including the Tazheran steppes (Sklyarov et al., 2010).

127 3. Methods

128
129 Fieldwork took place on 26th July 2006. pH and conductivity were measured *in situ*
130 using a Fisher Scientific accumet AP85 pH/conductivity meter. The pH of the surface water
131 was 9.0 pH units, and conductivity was 790 $\mu\text{S}/\text{cm}$. Due to time constraints, it was not
132 possible to conduct a detailed bathymetry of the lake, although a Plastimo Echotest II
133 handheld depth sounder was used to estimate the deepest region at 3.10 m, from where coring
134 was undertaken. A 71 mm diameter Livingstone core was initially extracted (44 cm length),
135 which maintained the surface sediment – water interface, followed by a second overlapping
136 Livingstone drive of 91 cm. Core location co-ordinates were 106°25'50.70"E, 52°41'14.54"N.

138 3.1 Chronology

139
140 Extracted lake sediments were highly humified and from many levels it was not
141 possible to obtain sizeable plant macrofossils for radiocarbon analyses. Radiocarbon dating of
142 humified sediments was instead performed on total organic carbon (TOC) from 5 bulk
143 sediment samples. *Potamogeton* seeds were isolated from a further four levels. All nine
144 samples were radiocarbon dated using accelerator mass spectrometry (AMS) at the Poznan
145 Radiocarbon Laboratory, Poland (Goslar *et al.*, 2004) (Table 1). The amount of radiocarbon
146 reservoir effect (i.e. shift towards older ages) was estimated on the basis of ¹⁴C dating
147 contemporary leaf sample of *Potamogeton* from the littoral region of Lake Khall. The result
148 of 105.58±0.33 pMC suggests a reservoir age of 100-200 years (Table 1). We have therefore
149 added the reservoir correction of 150±50 years to the age model for Lake Khall sediment
150 core.

151 Calibration of radiocarbon dates was undertaken using the Intcal09 calibration curve
152 (Reimer et al., 2009). The calibration was performed by “Bacon” software simultaneously to
153 building the calendar age scale for the whole core. In order to produce the age-depth model
154 this programme simulates the accumulation of deposit through small random increments, and
155 also takes into account the limitations on accumulation rate and its variability (Blaauw and
156 Christen, 2011). Although some of the obtained ¹⁴C dates can clearly be regarded as outliers,
157 all results of radiocarbon dating were included in the modeling performed for Lake Khall.
158 Additionally, the sampling year AD 2006 was assigned to the depth 0 and AD 1963 at 6.25
159 cm, identified on the basis of ¹³⁷Cs peak. The age-depth model was calculated with 20
160 sections. The *a priori* information for accumulation rate was set as a gamma distribution with
161 mean 30 yrs/cm and shape 2, and a beta distribution with strength 4 and mean 0.7 was fixed
162 for the accumulation variability, following the recommendation by Blaauw and Christen
163 (2011). The age-depth model resulting from 2640000 iterations is presented in Figure 2.

164 The uppermost 36 cm of sediment were also dated using ²¹⁰Pb, a naturally-produced
165 radionuclide that has been extensively used in the dating of recent sediments (Appleby, 2001)
166 and ¹³⁷Cs, an artificially produced radionuclide, introduced to the study area by atmospheric
167 fallout from nuclear weapons testing. Core sub-samples were counted on a Canberra well-
168 type ultra-low background HPGe gamma ray spectrometer to determine the activities of ²¹⁰Pb,
169 ¹³⁷Cs and other gamma emitters. Spectra were accumulated using a 16K channel integrated
170 multichannel analyzer and analysed using the Genie 2000 system. Energy and efficiency
171 calibrations were carried out using bentonite clay spiked with a mixed gamma-emitting
172 radionuclide standard, QCYK8163, and checked against an IAEA marine sediment certified
173 reference material (IAEA 135). The ²¹⁰Pb_{excess} activity was estimated by subtraction of the
174 average value of ²¹⁰Pb activity in deeper core samples (14 Bq/kg), where total ²¹⁰Pb activities
175 had fallen to virtually constant values and so approximate the “background” or supported
176 ²¹⁰Pb activity. Sediment accretion rates were determined using the Constant Flux, Constant
177 Sedimentation (CF-CS) model of ²¹⁰Pb dating, where the sedimentation rate is given by the

178 slope of the least squares fit for the natural log of the $^{210}\text{Pb}_{\text{excess}}$ activity versus depth
179 (Krishnaswami et al., 1971; Robbins, 1978).

180

181 3.2 Pollen analysis

182

183 Twenty-nine 1 cm³ sediments were processed for pollen analysis using standard
184 laboratory methods, including HCl and KOH treatments, heavy-liquid separation and
185 subsequent acetolysis (Berglund and Ralska-Jasiewiczowa, 1986). Pollen and spores were
186 mounted in glycerin and counted using light microscopy at $\times 400$ – $\times 1000$ magnification.
187 Identification of fossil pollen and spores was assisted with the use of regional pollen atlases
188 (Kuprianova and Alyoshina, 1972; Bobrov et al., 1983; Moore et al., 1991) and the reference
189 collection held at the Institute of the Earth Crust, Irkutsk. Between 176 and 518 terrestrial
190 pollen grains were counted at each level (304 on average). Relative abundances of individual
191 taxa were based on the sum of all terrestrial pollen grains. *Haploxylon*-type pine pollen (*Pinus*
192 *sibirica*, *Pinus pumila*) were separated from *Diploxylon*-type pine pollen (*Pinus sylvestris*)
193 based on the position of the sacci in polar view. *Pediastrum* coenobia colonies contain
194 sporopollenin which allowed us to count them alongside pollen (e.g. Nielsen and Sørensen,
195 1992). *Pediastrum* relative abundances were calculated in relation to the total sum of
196 terrestrial pollen. We used the pollen-based biome reconstruction method and equation
197 presented in Prentice et al. (1996) and a regionally approved biome-taxon matrix (Tarasov et
198 al., 2009; Bezrukova et al., 2010), which assigns all selected pollen taxa to appropriate
199 biomes. All terrestrial pollen taxa from Lake Khall sediments were assigned to regional plant
200 functional types (PFTs) and biomes– see Tarasov et al. (2009) for full details. Quantitative
201 climate reconstructions were performed using best modern analogue (BMA) approach
202 (Overpeck et al., 1985; Guiot, 1990) previously applied to the Holocene pollen records from
203 Lake Baikal (Tarasov et al., 2007) and Lake Kotokel (Tarasov et al., 2009). A reference
204 modern dataset based on the global climate averages (New et al., 2002) and extensive modern
205 surface pollen data from northern Eurasia, with a good representation of the Lake Baikal
206 region (see Tarasov et al., 2005 for details). Reconstructions undertaken were annual
207 precipitation (Pann), mean July temperatures (T_w , also referred to here as mean temperature
208 of the warmest month), and mean January temperature (T_c , also referred to here as mean
209 temperature of the coldest month).

210

211 3.3 Ostracods

212

213 Forty samples were processed for ostracod determinations. Wet sediment samples
214 were dispersed in tap water overnight and then gently sieved through a 250 μm mesh. The
215 coarse residues were dried at 105°C. All of the ostracod shells were picked from these
216 residues under a low-power binocular microscope using a fine (4/0) moistened paintbrush,
217 sorted into taxonomic groups and stored in micropalaeontological slides. Results are
218 expressed in numbers of valves per unit weight of sediment.

219

220 3.4 Mineral Magnetism

221

222 At least 1.5 g of freeze-dried sediment from forty-one samples was packed into
223 plastic magnetism sample pots. Low-frequency and high-frequency magnetic susceptibility
224 was measured for each sample using a Bartington MS2 Magnetic Susceptibility meter.

225

226 3.5 Particle size

227

228 Particle-size analysis was undertaken on the < 2 mm fraction of sediment from 40
229 samples. In practice, most of the sediment from the core was less than 2 mm diameter, so the
230 grain-size analyses are essentially bulk-sample determinations. Each sample was dispersed in
231 water, sieved through a 2 mm mesh and then disaggregated ultrasonically prior to analysis
232 using a Malvern Mastersizer laser particle-sizer. The results were processed using

233 GRADISTAT (Blott and Pye, 2001). For plotting purposes, we used the grain-size statistics
234 produced from the Folk and Ward (1957) method.

235

236 3.6 X-ray fluorescence (XRF) spectrometry analysis

237

238 Up to 2 g of freeze dried sediment was finely ground and compressed into 25 mm
239 deep polythene sample pots for XRF analysis of fortyone samples. Samples were subjected to
240 gamma photons from a silicon (lithium) semi-conductor detector for 240 s each, using a
241 Spectro Xlab 2000 energy dispersive XRF spectrometer. Calibration was conducted with two
242 known sediment standards of Buffalo River Sediment.

243

244 3.7 Statistical Analyses

245

246 Detrended correspondence analysis (DCA) was initially undertaken to establish the
247 magnitude of vegetation turnover. Relative abundance data were $\log(x+1)$ transformed in
248 order to stabilize species variance and rare species were down-weighted. The axis 1 gradient
249 length (standard deviation units) was 1.049, indicating that linear ordination techniques were
250 more appropriate for analyses. Principal components analysis (PCA) with symmetric scaling
251 of the ordination scores to optimise scaling for both samples and species was undertaken
252 (Gabriel, 2002). Species data were $\log(x+1)$ transformed and both species and samples were
253 centred to give a log-linear contrast PCA, appropriate for closed relative abundance data
254 (Lotter and Birks, 1993). XRF data were analysed using PCA with samples centred and
255 standardised. Significance of PC axes were tested with a broken stick model (Jollifer, 1986)
256 using BSTICK v1.0 (Line and Birks, 1996). Compositional change in the palynological data
257 (β -diversity) was estimated using detrended canonical correspondence analysis (DCCA) with
258 the data constrained using dates obtained from the age-depth model (Birks, 2007). All
259 ordination analyses were undertaken using Canoco v. 4.5 (ter Braak and Šmilauer, 2002).
260 Monte Carlo permutation tests for temporally ordered data were used to determine
261 significance levels ($n = 499$). Stratigraphical profiles were constructed using C2 Data
262 Analysis Version 1.5.1 (Juggins, 2007). Stratigraphical zones for each proxy were delimited
263 by optimal partitioning (Birks and Gordon, 1985) using the unpublished programme ZONE
264 (version 1.2) (Juggins, 1991).

265

266 4. Results

267

268 4.1 Core description and chronology

269

270 The core consisted mainly of homogenous, silty clay sediment between 0 – 76 cm
271 (colour 5Y-4/1-2), with the bottom sediments (76 – 91 cm; colour 10YR-3/1) packed full of
272 broken bivalve shells. The age-depth model for Lake Khall shows that the core spans the past
273 ca. 5.2 cal ka BP (i.e calibrated years before AD 1950, taken as present, are consistently used)
274 (Fig. 2). Although the sedimentation rate underwent temporal variability, some distinct
275 sections can be distinguished, for which the sedimentation rate was relatively constant. For
276 the uppermost section from 0 to 8 cm (ca. 10 cal BP) the average sedimentation rate derived
277 from the Bacon model was 1.48 ± 0.25 mm/year, which is in accordance with the number
278 obtained on the basis of ^{210}Pb measurements (1.11 ± 0.44 mm/year). The mean accumulation
279 rate for the section between 8 cm (10 cal BP) and 74 cm (ca. 2.6 cal ka BP) was 0.36 ± 0.02
280 mm/year. The oldest part of the sediment was characterized by lower sedimentation rate,
281 0.16 ± 0.043 mm/year.

282

283 4.2 Pollen stratigraphy

284

285 Taiga was the dominant biome throughout the sequence (Fig. 3) suggesting the record
286 reflects the regional ‘forest’ signal rather than only the local ‘steppe’ one. Compositional
287 turnover in the palynological data was high (β -diversity=1.281), although greatest change

288 occurred between 5.15 – 2.48 cal ka BP, with a very rapid change between 2.75 – 2.48 cal ka
 289 BP (Fig 6). Between 1.76 – 0.84 cal ka BP there was very little change in vegetation
 290 composition, but variability increased markedly from ca. AD 1800 to the present. Only PCA
 291 axis 1 was significant and accounted for 71.1% of variation in the species data. Three zones
 292 were delimited within the pollen stratigraphy (Fig. 3).

- 293 • Khall-3 (91 – 73.5 cm; 5.15 - 2.61 cal ka BP) was characterised by highest abundances of
 294 *Betula sect. Albae* (25-50%) and *Artemisia* (10-19%). *Pinus sibirica* percentage values,
 295 initially very high at the very base of the profile (25%), declined abruptly to 3 % and then
 296 increased to 10-13% again. *Pinus sylvestris* was initially present in only very low
 297 abundances (3-4%) at the base of the profile and quickly increased, reaching up to 36-
 298 41% in upper part of this zone. *Picea obovata* and *Alnus fruticosa* reached their highest
 299 values (up to 5%) in this zone.
- 300 • Khall-2 (73.5 – 13.25 cm; 2.61 – 0.15 cal ka BP [ca. AD 1800]) was dominated by *P.*
 301 *syvestris* pollen, with values fluctuating between 60-84%. *P. sibirica* was also well
 302 represented (10-25%), and contribution from *Artemisia* varied between 0.5-9%. *Alnus*
 303 *fruticosa* pollen was absent or present in low abundances. *Picea* percentages were also
 304 generally low and did not exceed 3%.
- 305 • Khall-1 (13.25 - 0 cm; ca. AD 1800 – AD 2006) had a pollen composition similar to
 306 Khall-2, with slightly lower and fluctuating percentage values of *P. sylvestris* and slightly
 307 higher abundances of *B. sect. Albae* and Cyperaceae pollen. Within this zone *Pediastrum*
 308 algae spores appeared for the first time in the record, and rapidly increased to very high
 309 abundances.

310

311 4.3 Ostracods

312

313 We only present preliminary results here: detailed taxonomic and palaeoecological
 314 accounts of the ostracod assemblages will follow in a future publication. The ostracod
 315 assemblages were fairly low diversity (<10 species in total) and dominated by a member of
 316 the genus *Limnocythere*, which has yet to be identified to specific level (Fig. 4). Other taxa
 317 present include *Candona* spp., *Pseudocanadona* spp., *Cyclocypris* sp., *Cypris* sp., *Ilyocypris*
 318 sp. and *Potamocypris* sp. as well as several others that remain unidentified. In most of the
 319 core levels examined, adult and juvenile shells were found. Concentrations varied from about
 320 300 to less than 2 valves per gram of sediment. Concentrations were greatest in the basal 10
 321 cm of the core, declining above this. Candonids were absent above 2.10 cal ka BP. A varying
 322 proportion of the valves displayed a black coating. Energy dispersive spectroscopy (EDS)
 323 analysis under a scanning electron microscope suggested that the coating was non-metallic
 324 but laser Raman determinations were inconclusive.

325

326 4.4 Mineral Magnetism

327

328 Low field magnetic susceptibility measurements ranged between 0.1 - 4.7 10⁻⁵ SI
 329 (Fig. 5). Values increased by small amount from the base of the core up to ca. 2.8 cal ka BP
 330 (2 – 2.6 10⁻⁵ SI). There was a substantial increase in values between ca. 2.6 – 2.1 cal ka BP
 331 from 2.6 – 4.3 10⁻⁵ SI. Values showed almost no change between 1.4 – 1.0 cal ka BP, after
 332 which they declined to the top of the profile, with very rapid decline after AD 1800.

333

334 4.5 Particle Size

335

336 Mean particle size (Mz; μm) ranged between 12.7 – 48.3 μm) (mean = 20.6; median
 337 17.6). Five peaks greater than mean Mz occurred at 5.12, 2.52, 1.88, 0.79 cal ka BP and AD
 338 1925 (Fig 5). Sorting of the grain size distributions ranged between 3.2 and 7.1 μm (mean =
 339 3.9; median 3.7). Five sorting peaks greater than the mean occurred at identical times as peaks
 340 in Mz. Almost all skewness values were negative (mean = -0.1; median = -0.1), except for 5
 341 positive values that occurred at the same times as high values for mean grain size and sorting.

342 Kurtosis (mean = 1.0; median = 1.0) exhibited a different pattern from other grain size
343 parameters. Values were above average between 5.12 – 3.03 cal ka BP, and declined to lowest
344 value at 2.52 cal ka BP, when values of other particle size proxies increased. But peaks in
345 kurtosis did co-occur at 1.88, 0.79 cal ka BP and 1925 AD.

346 347 4.6 XRF spectrometry analysis 348

349 Selected elements are presented in Figure 7. Ti, Al and K increased from 5.08 cal -
350 1.80 cal ka BP. Between 1.80 – 0.80 cal ka BP values showed little variation, and then they
351 declined up to ca. AD 1950. The rate of decline increased at the top of zone Khall-2, from
352 0.12 ka BP, concomitant with rapid increase in sedimentation rate and decline in magnetic
353 susceptibility values. Only PCA axis 1 was significant, accounting for 73.8% of variance in
354 geochemical data. This axis was driven by a strong gradient between high Ca and Sr
355 concentrations at the bottom of the core, and high concentrations of most other elements
356 between ca. 1.90 – 0.50 cal ka BP (notably Fe, Y, Zn, Rb, K, Ti, Cu and Al) (Fig. 6).
357 Although axis 2 was insignificant, elevated concentrations of S and Cl were especially
358 abundant in the uppermost sediments.
359

360 361 5. Discussion 362

363 Taiga biome dominated the vegetation reconstruction from the Ol'khon region since
364 at least 5.2 ka BP. However, compositional turnover was very significant; β -diversity values
365 were considerably higher than for longer Holocene sequences in other boreal regions such as
366 southern Norway (Birks, 2007) and the eastern Sayan Mountains (Mackay et al., 2012). This
367 suggests that the semi-arid, Ol'khon region was more sensitive to climate variability and
368 environmental change than other boreal regions with higher precipitation. Such sensitivity
369 was responsible for major directional shifts during the past 5.2 cal ka in Lake Khall and the
370 surrounding region. DCCA and zonation analyses delimited most rapid periods of vegetation
371 change at 2.74 – 2.48 cal ka and after AD 1800. Pollen assemblage composition showed a
372 progressive decrease in birch pollen and shift to a predominance of Scots pine pollen between
373 5.15–2.48 cal ka, which drove overall compositional turnover. Scots pine produces vast
374 amounts of pollen, and once established, it dominates pollen assemblages. The numerical
375 scores of the taiga biome (Fig. 3) demonstrated minor fluctuations, but did not show
376 decreasing or increasing trend through the whole record. Therefore, the increase in arboreal
377 pollen percentages between 2.75 – 2.48 cal ka BP likely does not imply greater regional
378 afforestation, nor any decrease in steppe communities, but are indicative of change in forest
379 composition, with the spread of eurythermic and drought resistant Scots pine rather than
380 noticeable spread in regional woody cover. These findings are in line with the woody cover
381 reconstruction derived from Lake Kotokel pollen records on the opposite shore of Lake
382 Baikal (Fig. 1) (Tarasov et al., 2009; Bezrukova et al., 2010).
383

384 5.1 Mid-Holocene environmental change 385

386 Up to 4.5 cal ka BP, forest-steppe communities dominated local vegetation in
387 Ol'khon region, especially tree birches (*Betula sect. Albae*), *Artemisia* and *Chenopodiaceae*
388 taxa. Reconstructed temperature of the coldest month and annual precipitation were highest
389 during this period. Owing to the lack of formal identification of the ostracod species,
390 interpretations of the assemblages remain circumspect at this stage, although we can say that
391 assemblages were deposited *in situ*, because in most of the core levels examined, both adult
392 and juvenile shells were found. However, candonids generally only tolerate low salinity
393 waters (Holmes et al., 2010) and the Lake Khall assemblage suggests that the lake was fresher
394 in the past. The geochemical record also provides evidence for a fresher lake in the past; low
395 Sr/Ca ratios indicate low lake-water salinity (Marshall, 1969). Detrital transport from the
396 catchment into the lake are represented by e.g. Ti, Al and K, and these elements were lowest

397 when precipitation was highest. Ca on the other hand may come from both authigenic
398 production within the lake and from detrital flux (e.g. Wünnemann et al., 2010). In order to
399 distinguish between these two processes we use the Ca/Al ratio, which at the base of the core
400 was very high (60), indicative of high authigenic production. High production occurs at the
401 same time as highest concentrations of ostracods, and shell remains of a, as yet unidentified,
402 bivalve. We have as yet to characterise mineralogy of the sediments (e.g. using XRD) but low
403 K/Rb and high Ti/K ratios suggest dominance of clays and micas, although feldspars became
404 more important after 3.59 cal ka BP. Elsewhere in the Lake Baikal region, other records of
405 pollen-inferred annual precipitation were also high (e.g. Tarasov et al., 2007; Tarasov et al.,
406 2009), as was isotopic evidence for elevated precipitation-dominated discharge into Lake
407 Baikal (Mackay et al., 2011; Fig 8). Further afield, isotopic records from Dongge Cave in
408 southern China (Fig 8) were indicative of strong East Asian Summer Monsoon (EASM)
409 linked to relative high summer insolation (Wang et al., 2005).

410 Between ca. 4.4 – 2.8 cal ka BP, the pollen record is poorly resolved. However, there
411 was a significant expansion of Scots pine (*P. sylvestris*) and, to a lesser extent, Siberian pine
412 (*P. sibirica*) (a major component of dark, coniferous taiga), concomitant with a decline in
413 deciduous forest. The expansion of Scots pine occurred substantially later than at
414 neighbouring regions e.g. Lake Hovsgöl (10.0 cal ka BP; Prokopenko et al., 2007), Altai
415 Mountains, (9.5 cal ka BP, Blyakharchuk et al., 2004), Eastern Sayan Mountains (9.1 cal ka
416 BP, Mackay et al., 2012), southern Lake Baikal (7 cal ka BP, Demske et al., 2005) and Lake
417 Kotokel (ca. 6.9 - 6.4 cal ka BP (Bezrukova et al., 2008; Shichi et al., 2009). The expansion
418 of Scots pine in Ol'khon is in close agreement with the expansion of Scots pine to the north of
419 Lake Baikal (5.2 cal ka BP, Bezrukova et al., 2006), highlighting that distinct regional
420 differences exist in the spread of conifer forest to coastal regions of Lake Baikal. The period
421 of conifer expansion in Ol'khon region occurred during a period of increasing aridity, as
422 inferred from several of the proxies studied. For example, Sr/Ca ratios indicate a progressive
423 increase in salinity of Lake Khall, likely linked to reductions in pollen-inferred precipitation
424 anomalies, while pollen-inferred temperatures remained above values experienced in recent
425 decades (Fig. 8). Detrital input (inferred from Al, Ti and K) also increased at this time. Given
426 the similarity between PCA of the vegetation and geochemistry, it is likely that both were
427 influenced by the same drivers. Elsewhere, $\delta^{18}\text{O}_{\text{diatom}}$ showed a marked decline during this
428 period, indicative of a decline in the proportion of rain-fed discharge into Lake Baikal
429 (Mackay et al., 2011; Fig. 8). The shift to a more arid climate was also reflected further afield
430 in the weakening of the EASM (Wang et al., 2005; Fig. 8).

431

432 5.2 Abrupt environmental change

433

434 Compositional turnover in vegetation communities was greatest between 2.75 – 2.48
435 cal ka BP, which continued to change up to 1.87 cal ka BP, linked to the maximum expansion
436 of dark coniferous taiga. Particle size characteristics in Lake Khall show that they were
437 generally very poorly sorted, i.e. they had not undergone efficient sorting before their burial
438 into the bottom sediments, which is common for shallow lakes (Mischke et al., 2010). One of
439 the largest peaks in mean particle size occurred at 2.52 cal ka BP, which was likely caused by
440 strong aeolian influx because these large particles were also extremely unsorted (Fig. 5).
441 Pollen-inferred annual precipitation anomalies dropped rapidly, and values remained low,
442 below that of the present day, for much of the remainder of the Holocene (Fig. 8). There was
443 also a marked decline in mean temperature of coldest month, while mean temperatures of the
444 warmest month increased. The climate in the Ol'khon region therefore became more
445 continental. The start of these climatic and vegetation changes are coincident with a peak in
446 ice rafted debris material in North Atlantic sediments (IRD-2; Bond et al. 1997), which also
447 resulted in low $\delta^{18}\text{O}$ isotopic values in Lake Baikal and in Dongge cave, indicative of a
448 decline in proportion of rain-fed discharge into Lake Baikal (Mackay et al., 2011) and an
449 attenuated EASM (Wang et al., 2005) respectively.

450 Between 2.12 – 1.87 cal ka BP there was a significant decline in mean annual
451 precipitation and mean temperature of the coldest month but an increase in mean temperature

452 of the warmest month (Fig 8). Drier, more continental climate resulted in peak abundance of
453 Scots pine, which drove compositional turnover in the Ol'khon region. An increase in Sr/Ca
454 ratio suggested that chemical composition of the groundwater that feeds Lake Khall may have
455 become more saline, and this event may have caused the final decline in substantial numbers
456 of the ostracod *Candona* sp. Therefore it seems likely that the region underwent a period of
457 extreme drought, which led to a decline in ostracoda in general. The rapid increase in
458 sedimentation rate was concurrent with small peaks in particle size, perhaps indicative of
459 increased aeolian transport onto the lake.

460

461 5.3 Late Holocene variability

462

463 Between ca. 1.9 – 0.7 cal ka BP, taxa indicative of cold coniferous forest declined and
464 steppe communities virtually disappeared from the record altogether, coincident with marked
465 increases in warmest month temperature anomalies. This period in general was characterised
466 by little vegetation compositional change, and stable input of catchment derived particles
467 (Figs. 3, 5, 7). Increased reconstructed summer and winter temperatures were likely linked to
468 increased northern hemisphere temperatures, as inferred from the GRIP borehole (Dahl-
469 Jensen et al., 1998) (Fig. 8). Elsewhere in the Lake Baikal region, steppe communities were
470 also less common (Tarasov et al., 2007), while high biogenic silica concentrations within
471 Lake Baikal sediments were indicative of high aquatic productivity (Prokopenko et al., 2007).
472 Peak reconstructed summer temperatures occurred between 1.33 – 0.77 cal ka BP, coincident
473 with the period known as both the Medieval Warm Period (MWP) and Medieval Climate
474 Anomaly (MCA). This period is distinct because although temperatures in many regions were
475 warm (Mann et al., 2009) precipitation anomalies were also apparent in many regions in the
476 world (Stine, 1994), leading to severe drought in e.g. northern Europe (Helama et al., 2009)
477 and North America (Seager and Burgman, 2011). In the Ol'khon region, precipitation
478 anomalies were higher than the previous period of drought, but still lower than the present.
479 One of the few stratified deposits in the Lake Baikal region was excavated at Sagan-Zaba and
480 dated between 2.0 – 0.9 cal ka BP. These deposits were likely associated with pastoralists,
481 and although we are not able to say if the evidence of pastoralism was linked to a particularly
482 quiescent period of environmental change, warmer summer and milder winter temperatures
483 may have been conducive to a pastoral way of life.

484

485 For a short period between ca. 0.77 – 0.45 cal ka BP, local climate in the Ol'khon
486 region became wetter and substantially colder, leading to an increase in *P. sibirica*, *Picea*
487 *obovata* and sedge pollen. *P. obovata* (Siberian spruce) is characteristic of soils with elevated
488 moisture content, and likely represents real increases in tree abundance close to the lake
489 (Bezrukova et al., 2005). However, there did not appear to be a substantial influence on Lake
489 Khall itself – Sr/Ca ratios continued to increase, while ostracods only showed small increases
490 in concentration. It is noteworthy that candonids did not recolonise the lake in any substantial
491 numbers, and that black coatings on the ostracod valves almost disappeared. On the basis of
492 the EDS and laser Raman determinations detailed in section 4.3, it was assumed that the
493 coatings were organic and indicative of reducing conditions in the upper layers of the
494 sediment following death of the ostracods. Blackened valves dominated the lower part of the
495 core, and were less common above 0.68 cal ka BP, suggesting a significant change in the
496 ventilation of the lake after this time. Further work still needs to be done to determine the
497 nature of the black coatings. Wetter climate has also been reconstructed from peat bog
498 sequences from the northern shore of Lake Baikal (Bezrukova et al., 2006), and further afield
499 in the Eastern Sayan mountains (Mackay et al. 2012). This period is coincident with IRD0 in
500 North Atlantic sediments and attenuation of the EASM (Wang et al., 2005; Fig 8), and is
501 concurrent with the Little Ice Age. Young moraines, associated with re-advancing glaciers at
502 this time, can be found in the Sayan Mountains (Ivanovsky and Panychev, 1978 in
503 Shahgedanova et al., 2002), indicative of cooler, regional environments (Krenke and
504 Chernavskaya, 2002). Chironomid-inferred temperatures from lake ESM-1 in the Eastern
505 Sayan Mountains also showed a distinct cooling (Mackay et al., 2012).

506 Since ca. AD 1845, the increase in deciduous forest was linked to increased pollen-
507 inferred precipitation and pollen-inferred temperature anomalies of the coldest and warmest
508 months. The most striking change in the palynological record however, is the rapid increase
509 in *Pediastrum* algae. *Pediastrum* belongs to the Chlorophyceae green algae, and is often
510 characteristic of more nutrient rich waters. Palaeoenvironmental interpretations from
511 *Pediastrum* records in lake sediments are not straightforward. Several studies tie the presence
512 of *Pediastrum* to high lake levels in the semi-arid regions of e.g. Inner Mongolia (Jiang et al.,
513 2006) and NE Tibetan Plateau (Zhao et al., 2007). In southern Scandinavia, increased
514 concentrations of *Pediastrum* coenobia occurred during periods of warmer climate and
515 increased lacustrine productivity (Sarmaja-Korjonen et al., 2006; Panizzo et al., 2008). In
516 Lake Khall, increasing *Pediastrum* was coincident with increases in temperature of the
517 coldest month and annual precipitation. During this period there was a rapid increase in
518 sediment accumulation rate, the fastest for the past 5 ka, concomitant with a rapid decline in
519 low field initial magnetic susceptibility measurements. This suggests that there was a decline
520 in magnetisable sediments, possibly related to increased organic content and presence of algal
521 growth. The increase in *Pediastrum* sp. therefore is likely indicative of a more nutrient rich
522 lake. Animal husbandry intensified in the Lake Baikal region at this time because of the
523 influx of Russian populations (Tarasov et al., 2007). Local populations later undertook tree-
524 felling (Sizykh, 2007), and although there is limited pollen evidence of anthropogenic
525 activities, impacts on lacustrine ecosystems could be expected.

526 527 **6. Conclusions**

528
529 A multiproxy study of a small, shallow lake in the Ol'khon region of Lake Baikal was
530 undertaken to determine climatic and human impacts on the landscape over the mid- to late-
531 Holocene. We could only relate the significant turnover in vegetation composition to climate
532 variability, and we found no evidence for anthropogenic activity despite the region having a
533 long history of pastoralism. Geochemical evidence suggested that Lake Khall was once more
534 fresh than it is today, and that over the study period, groundwater feeding the lake became
535 more saline. The change in chemical composition had a negative impact on aquatic fauna by 2
536 cal ka BP. Pollen based reconstructions from Lake Kotokel, a satellite to Lake Baikal
537 (Tarasov et al., 2009) and regional climate modelling (White and Bush, 2010) exhibited
538 similar trends to reconstructions from Lake Khall. For example, general trends demonstrated
539 a decline in atmospheric precipitation and increase in continentality. The decrease in
540 precipitation was accompanied by the changes in its seasonality, i.e. late Holocene
541 strengthening of Westerlies in the region caused relative increase in winter (snow)
542 accumulation. This feature together with drier summer conditions favoured the spread of
543 drought resistant Scots pine. Reconstructed cool, moist conditions during the Little Ice Age
544 are consistent with other palaeolimnological records, highlighting the regional nature of the
545 response. Proxy records from Lake Khall also show a period of relative stability concurrent
546 with the Medieval Climate Anomaly and a period of abrupt change between 2.75 – 2.48 cal
547 ka BP, concurrent with influence from IRD-2 event in the north Atlantic. Finally, although
548 human impact could not be determined from the terrestrial pollen record, preserved
549 *Pediastrum* colonies may be indicative of a major recent phase of human impact as numbers
550 of pastoralists migrated into the region in the last 100 years.

551 552 **Acknowledgements**

553 We gratefully acknowledge funding through the Baikal Archaeology Project,
554 supported by the Major Collaborative Research Initiative (MCRI) programme of the Social
555 Sciences and Humanities Research Council of Canada. Thanks are given to Cath D'Alton for
556 help in preparing figures and to Holly Watson for undertaking magnetic susceptibility
557 measurements and particle size analysis.

560
561
562
563
564
565
566
567
568
569
570
571
572
573
574
575
576
577
578
579
580
581
582
583
584
585
586
587
588
589
590
591
592
593
594
595
596
597
598
599
600
601
602
603
604
605
606
607
608
609
610
611
612
613

References

- Appleby, P.G., 2001. Chronostratigraphic techniques in recent sediments. In: Last, W.M., Smol, J.P. (Eds.) *Tracking Environmental Change Using Lake Sediments, Volumes 1*. Kluwer, Dordrecht, pp. 171-203
- Atlas Baikala (Baikal Atlas) 1993. Federal Service of Surveying and Cartography, Moscow. 159 pp. In Russian.
- Berger A., Loutre M.F., 1991. Insolation values for the climate of the last 10 million years. *Quaternary Science Reviews* 10, 297-317.
- Berglund, B.E., Ralska-Jasiewiczowa, M., 1986. Pollen analysis and pollen diagrams. In: Berglund, B.E. (Ed.), *Handbook of Holocene Palaeoecology and Palaeohydrology*, Interscience, New-York, pp. 455-484.
- Bezrukova, E.V., Abzaeva, A.A., Letunova, P.P., Kulagina, N.V., Vershinin, K.E., Belov, A.V., Orlova, L.A., Danko, L.V., Krapivina, S.M., 2005. Post-glacial history of Siberian spruce (*Picea obovata*) in the Lake Baikal area and the significance of this species as a paleo-environmental indicator. *Quaternary International* 136, 47-57.
- Bezrukova, E.V., Belov, A.V., Abzaeva, A.A., Letunova, P.P., Orlova, L.A., Sokolova, L.P., Kalugina, N.V., Fisher, E.E., 2006. First high-resolution dated records of vegetation and climate changes on the Lake Baikal northern shore in the middle-late Holocene. *Doklady Earth Sciences* 411, 1331-1335.
- Bezrukova, E.V., Krivonogov, S.K., Takahara, H., Letunova, P.P., Shichi, K., Abzaeva, A.A., Kalugina, N.V., Zabelina, Yu. S., 2008. Lake Kotokel as a stratotype for the Lake Glacial and Holocene southeastern Siberia. *Doklady Earth Sciences* 420, 658-663.
- Bezrukova, E.V., Tarasov, P.E., Solovieva, N., Krivonogov, S.K., Fiedal, F., 2010. Last glacial-interglacial vegetation and environmental dynamics in southern Siberia: chronology, forcings and feedbacks. *Palaeogeography, Palaeoclimatology, Palaeoecology* 296, 185-198.
- Birks, H.J.B., 2007. Estimating the amount of compositional change in late-Quaternary pollen stratigraphical data. *Vegetation History and Archaeobotany* 16, 197-202.
- Birks, H.J.B., Gordon, A.D., 1985. *Numerical methods in Quaternary pollen analysis*. Academic Press, London.
- Blaauw, M., Christen, J.A., 2011. Flexible paleoclimate age-depth models using an autoregressive gamma process. *Bayesian Analysis* 6, 457-474.
- Blott, S.J., Pye, K., 2001. GRADISTAT: a grain size distribution and statistics package for the analysis of unconsolidated sediments. *Earth Surface Processes and Landforms* 26, 1237-1248.
- Blyakharchuk, T.A., Wright, H.E., Borodavko, P.S., van der Knaap, W.O., Amman, B., 2004. Late Glacial and Holocene vegetational changes on the Ulagan high-mountain plateau, Altai Mountains, southern Siberia. *Palaeogeography, Palaeoclimatology and Palaeoecology* 209, 259-279.
- Bobrov, A.E., Kuprianova, L.A., Litvintseva, M.V., Tarasevich, V.F., 1983. *Sporae Pteridophytorum et Pollen Gymnospermarum Monocotyledonearumque. Florae Partes Europaeae USSR*. Nauka, Leningrad. (in Russian).
- Bond, G., Showers, W., Cheseby, M., Lotti, R., Almasi, P., deMenocal, P., Priore, P., Cullen, H., Hajdas, I., Bonani, G., 1997. A pervasive millennial scale cycle in North Atlantic Holocene and glacial climates. *Science* 278, 1257-1256.
- Bronk Ramsey, C., 2009. Bayesian analysis of radiocarbon dates. *Radiocarbon* 51, 337-360.
- Dahl-Jensen, D., Mosegaard, K., Gundestrup, N., Clow, G.D., Johnsen, S.J., Hansen, A.W., Balling, N., 1998. Past temperatures directly from the Greenland Ice Sheet. *Science* 282, 268-271.
- Demske, D., Heumann, G., Granoszewski, W., Nita, M., Mamakowa, K., Tarasov, P.E., Oberhänsli, H., 2005. Late glacial and Holocene vegetation and regional climate variability evidenced in high-resolution pollen records from Lake Baikal. *Global and Planetary Change* 46, 255-279.

- 614 Folk, R.L., Ward, W.C., 1957. Brazos River bar: a study in the significance of grain size
615 parameters. *Journal of Sedimentary Petrology* 27, 3-26.
- 616 Gabriel, K.R., 2002. Goodness of fit of biplots and correspondence analysis. *Biometrika* 89,
617 423-436.
- 618 Goslar T., Czernik J., Goslar E., 2004. Low-energy ¹⁴C AMS in Poznan radiocarbon
619 Laboratory, Poland. *Nuclear Instruments and Methods in Physics Research B*, 223-
620 224, 5-11.
- 621 Guiot, J., 1990. Methodology of the last climatic cycle reconstruction from pollen data.
622 *Palaeogeography, Palaeoclimatology, Palaeoecology* 80, 49–69.
- 623 Helama, S., Merilainen, J., Tuomenvirta, H., 2009. Multicentennial megadrought in northern
624 Europe coincided with a global El Niño-Southern Oscillation drought pattern during
625 the Medieval Climate Anomaly. *Geology* 37, 175-178.
- 626 Holmes, J., Sayer, C.D., Liptrot, E., Hoare, D.J., 2010. Complex controls on ostracod
627 palaeoecology in a shallow coastal brackish-water lake: implications for
628 palaeosalinity reconstruction. *Freshwater Biology* 55, 2484-2498.
- 629 Jacobson, G.L., Jr, Bradshaw, R.H.W., 1981. The selection of sites for paleovegetational
630 studies. *Quaternary Research* 16, 80–96.
- 631 Jiang, W.Y., Guo, Z.T., Sun, X.J., Wu, H.B., Chu, G.Q., Yuan, B.Y., Hattée, C., Guiot, J.,
632 2006. Reconstruction of climate and vegetation changes of Lake Bayanchagan (Inner
633 Mongolia): Holocene variability of the East Asian monsoon. *Quaternary Research* 65,
634 411–420.
- 635 Jolliffe, I.T., 1986. *Principal components analysis*. Springer-Verlag, New York.
- 636 Juggins, S., 1991. ZONE, Version 1.2. University of Newcastle, Newcastle Upon Tyne, UK.
- 637 Juggins, S., 2007. C2 Version 1.5.1 Software for ecological and palaeoecological data
638 analysis and visualisation. Newcastle University, Newcastle upon Tyne, UK.
- 639 Krenke, A.N., Chernavskaya, M.M., 2002. Climate changes in the preinstrumental period of
640 the last millennium and their manifestations over the Russian Plain. *Izvestiya,*
641 *Atmospheric and Oceanic Physics* 38, S59-S79.
- 642 Krishnaswami, S., Lal, D., Martin, J.M., Meybeck, M., 1971. Geochronology of lake
643 sediments. *Earth and Planetary Science Letters* 11, 407-414.
- 644 Kuprianova, L.A., Alyoshina, L.A., 1972. Pollen and spores of the plants of the flora of the
645 European part of USSR. Nauka, Leningrad (in Russian).
- 646 Line, J.M., Birks, H.J.B., 1996. BSTICK Version 1.0. Unpublished computer program.
647 Botanical Institute, University of Bergen, Bergen.
- 648 Lotter, A.F., Birks, H.J.B., 1993. The impact of the Laacher See tephra on terrestrial and
649 aquatic ecosystems in the Black Forest, southern Germany. *Journal of Quaternary*
650 *Science* 8, 263-276.
- 651 Mackay, A.W., Swann, G.E.A., Brewer, T., Leng, M.J., Morley, D.W., Piotrowska, N.,
652 Rioual, P., White, D., 2011. A reassessment of Lateglacial–Holocene diatom oxygen
653 isotope records from Lake Baikal using a mass balance approach. *Journal of*
654 *Quaternary Science* 26, 627-634.
- 655 Mackay, A.W., Bezrukova, E.V., Leng, M.J., Meaney, M., Nunes, A., Piotrowska, N., Self,
656 A., Shchetnikov, A., Shilland, E., Taarasov, P., Wang, L., White, D., 2012. Aquatic
657 ecosystem responses to Holocene climate change and biome development in boreal
658 central Asia. *Quaternary Science Reviews* 41, 119-131.
- 659 Mann, M.E., Zhang, Z., Rutherford, S., Bradley, R.S., Hughes, M.K., Shindell, D., Ammann,
660 C., Faluvegi, G., Ni, F., 2009. Global signatures and dynamical origins of the Little
661 Ice Age and Medieval Climate Anomaly. *Science* 326, 1256-1260.
- 662 Marshall, F.C., 1969. Lower and Middle Pennsylvanian Fusulinids from the Bird Spring
663 Formation near Mountain Springs Pass, Clark County, Nevada. *Brigham Young*
664 *University Geology Studies* 16, 97-154.
- 665 Mischke, S., Zhang, C., Börner, A., Herzschuh, U., 2010. Lateglacial and Holocene variation
666 in Aeolian sediment flux over the northeastern Tibetan Plateau recorded by laminated
667 sediments of a saline meromictic lake. *Journal of Quaternary Science* 25, 162-177.
- 668 Moore, P.D., Webb, J.A., Collinson, M.E., 1991. *Pollen Analysis*. Blackwell Scientific

669 Publications, Osney Mead, Oxford.

670 Müller, G., Iron, G., Forstner, U., 1972. Formation and diagenesis of inorganic Ca-Mg
671 carbonates in the lacustrine environment. *Naturwissenschaften* 59, 158–64.

672 New, M., Lister, D., Hulme, M., Makin, I., 2002. A high-resolution data set of surface climate
673 over global land areas. *Climate Research* 21, 1–25.

674 Nielsen, H., Sørensen, I., 1992. Taxonomy and stratigraphy of lateglacial *Pediastrum* taxa
675 from Lysmosen, Denmark – a preliminary study. *Review of Palaeobotany and*
676 *Palynology* 74, 55–75.

677 Nomokonova, T., Losely, R.J., Goriunova, O.I., Weber, A., (in review). A freshwater old
678 carbon offset in Lake Baikal, Siberia and problems with the radiocarbon dating of
679 archaeological sediments: evidence from the Sagan Zaba II site. *Quaternary*
680 *International*

681 Nomokonova, T., Losely, R.J., Weber, A., Goriunova, L.I., Novikov, A.G., 2010. Late
682 Holocene subsistence practices among cis-Baikal pastoralists, Siberia:
683 zooarchaeological insights from Sagan-Zaba II. *Asian Perspectives* 49, 157-179.

684 Overpeck, J.T., Webb III, T., Prentice, I.C., 1985. Quantitative interpretation of fossil pollen
685 spectra, dissimilarity coefficients and the method of modern analogs. *Quaternary*
686 *Research* 23, 87–108.

687 Panizzo, V.N., Jones, V.J., Birks, H.J.B., Boyle, J.F., Brooks, S.J., Leng, M.J., 2008. A
688 multiproxy palaeolimnological investigation of Holocene environmental change,
689 between c. 10 700 and 7200 years BP, at Holebudalen, southern Norway. *The*
690 *Holocene* 18, 805-817.

691 Prentice, I.C., Guiot, J., Huntley, B., Jolly, D., Cheddadi, R., 1996. Reconstructing biomes
692 from palaeological data: a general method and its application to European pollen
693 data at 0 and 6 ka. *Climate Dynamics* 12, 185–194.

694 Prokopenko, A.A., Khursevich, G.K., Bezrukova, E.V., Kuzmin, M.I., Boes, X., Williams,
695 D.F., Fedenya, S.A., Kulagina, N.V., Letunova, P.P., Abzaeva, A.A., 2007.
696 Paleoenvironmental proxy records from Lake Hovsgol, Mongolia, and a synthesis of
697 Holocene climate change in the Lake Baikal watershed. *Quaternary Research* 68, 2-
698 17.

699 Ptitsyn, A.B., Reshetova, S.A., Babich, V.V., Daryin, A.V., Kalugin, I.A., Ovchinnikov,
700 D.V., Panizzo, V., Myglan, V.S., 2010. Palaeoclimate chronology and aridization
701 tendencies in the Transbaikalia for the last 1900 years. *Geography and Natural*
702 *Resources* 31, 144-147.

703 Reimer, P.J., Baillie, M.G.L., Bard, E., Bayliss, A., Beck, J.W., Blackwell, P.G., Bronk
704 Ramsey, C., Buck, C.E., Burr, G.S., Edwards, R.L., Friedrich, M., Grootes, P.M.,
705 Guilderson, T.P., Hajdas, I., Heaton, T.J., Hogg, A.G., Hughen, K.A., Kaiser, K.F.,
706 Kromer, B., McCormac, F.G., Manning, S.W., Reimer, R.W., Richards, D.A.,
707 Southon, J.R., Talamo, S., Turney, C.S.M., van der Plicht, J., Weyhenmeyer, C.E.,
708 2009. IntCal09 and Marine09 radiocarbon age calibration curves, 0–50,000 years cal
709 BP. *Radiocarbon* 51, 1111–50.

710 Robbins, J.A., 1978. Geochemical and geophysical applications of radioactive lead. In:
711 Nriagu, J.O. (Ed.) *Biogeochemistry of Lead in the Environment*. Elsevier Scientific,
712 Amsterdam, 285-393.

713 Sarmaja-Korjonen, K., Seppänen, A., Bennike, O., 2006. *Pediastrum* algae from the classic
714 late glacial Bølling Sø site, Denmark: response of aquatic biota to climate change.
715 *Review of Palaeobotany and Palynology* 138, 95–107.

716 Seager, R., Burgman, R.J., 2011. Medieval hydroclimate revisited. *PAGES news* 19, 10-12.

717 Seppä, H., Bennett, K.D., 2003. Quaternary pollen analysis: recent progress in palaeoecology
718 and palaeoclimatology. *Progress in Physical Geography* 27, 548-579.

719 Shahgedanova, M., Mikhailov, N., Larin, S., Bredikhin, A., 2002. The mountains of southern
720 Siberia. In: Shahgedanova, M. (Ed.) *The Physical Geography of Northern Eurasia*.
721 OUP, Oxford, pp 314-349.

- 722 Shichi, K., Takahara, H., Krivonogov, S.K., Bezrukova, E.V., Kashiwaya, K., Takehara, A.,
723 Nakamura, T., 2009. Late Pleistocene and Holocene vegetation and climate records
724 from Lake Kotokel, central Baikal region. *Quaternary International* 205, 98-110.
- 725 Sizykh, A.P., 2007. Models of taiga-steppe communities on the western coast of Lake Baikal.
726 *Russian Journal of Ecology* 38, 234-237
- 727 Sklyarov, E.V., Solotchina, E.P., Vologina, E.G., Ignatova, N.V., Izokh, O.P., Kulagina,
728 N.V., Sklyarova, O.A., Solotchin, P.A., Stolpovskaya, V.N., Ukhova, N.N.,
729 Federovskii, V.S., Khlystov, O.M., 2010. Detailed Holocene climate record from the
730 carbonate section of saline Lake Tsagan-Tyrm (West Baikal area). *Russian Geology
731 and Geophysics* 51, 237-258.
- 732 Sklyarova, O.A., Sklyarov, E.V., Fedorovskii, V.S., 2002. Structural control of location and
733 water chemistry of lakes and springs in the Ol'khon region. *Russian Geology and
734 Geophysics* 43, 732-745.
- 735 Stine, S., 1994. Extreme and persistent drought in California and Patagonia during Medieval
736 time. *Nature* 369, 546-549.
- 737 Sugita, S., 1994. Pollen representation of vegetation in Quaternary sediments: theory and
738 method in patchy vegetation. *Journal of Ecology* 82, 881-97.
- 739 Tarasov, P., Granoszewski, W., Bezrukova, E., Brewer, S., Nita, M., Abzaeva, A.,
740 Oberhänsli, H., 2005. Quantitative reconstruction of the Last Interglacial vegetation
741 and climate based on the pollen record from Lake Baikal, Russia. *Climate Dynamics*
742 25, 625-637.
- 743 Tarasov, P., Bezrukova, E., Karabanov, E., Nakagawa, T., Wagner, M., Kulagina, N.,
744 Letunova, P., Abzaeva, A., Granoszewski, W., Riedel, F., 2007. Vegetation and
745 climate dynamics during the Holocene and Eemian interglacials derived from Lake
746 Baikal pollen records. *Palaeogeography, Palaeoclimatology and Palaeoecology* 252,
747 440-457.
- 748 Tarasov, P.E., Bezrukova, E.V., Krivonogov, S.K., 2009. Late Glacial and Holocene changes
749 in vegetation cover and climate in southern Siberia derived from a 15 kyr long pollen
750 record from Lake Kotokel. *Climate of the Past* 5, 285-295.
- 751 ter Braak, C.J.F., Šmilauer, P., 2002. CANOCO reference manual and user's guide to
752 CANOCO for Windows: Software for Canonical Community Ordination version 4.5.
753 Microcomputer Power, Ithaca, New York.
- 754 Thompson, R., Oldfield, F., 1986. *Environmental Magnetism*. George Allen and Unwin,
755 London, 227 pp.
- 756 Wang, Y., Cheng, H., Edwards, R.L., He, Y., Kong, X., An, Z., Wu, J., Kelly, M.J., Dykoski,
757 C.A., Li, X., 2005. The Holocene Asian monsoon: links to solar changes and North
758 Atlantic climate. *Science* 308, 854-857.
- 759 Weber, A.W., Link, D.W., Katzenberg, M.A., 2002. Hunter-gather culture change and
760 continuity in the middle Holocene of the cis-Baikal, Siberia. *Journal of
761 Anthropological Archaeology* 21, 230-299.
- 762 Weber, A.W., Katzenberg, M.A., Schurr, T.G., (Eds.), 2010. *Prehistoric Hunter-Gatherers of
763 the Baikal Region, Siberia: Bioarchaeological Studies of Past Lifeways*. University of
764 Pennsylvania Press, Philadelphia, USA.
- 765 White D., Bush A.B.G., 2010. Holocene climate, environmental variability and Neolithic
766 biocultural discontinuity in the Lake Baikal region. In *Prehistoric Hunter-Gatherers of
767 the Baikal Region, Siberia: Bioarchaeological Studies of Past Lifeways*, Weber AW,
768 Katzenberg MA, Schurr TG (eds) Pennsylvania; University of Pennsylvania Museum
769 Press: 1-26
- 770 Wünneman, B., Demske, D., Tarasov, P., Kotlia, B.S., Reinhardt, C., Bloemendal, J.,
771 Diekmann, B., Hartmann, K., Krois, J., Riedal, F. Arya, N., 2010. Hydrological
772 evolution during the last 15 kyr in the Tso Kar lake basin (Ladakh, India), derived
773 from geomorphological, sedimentological and palynological records. *Quaternary
774 Science Reviews* 29, 1138-1155.

775 Zhao, Y., Yu, Z., Chen, F., Ito, E., Zhao, C., 2007. Holocene vegetation and climate history at
776 Hurleg Lake in the Qaidam Basin, northwest China. *Review of Palaeobotany and*
777 *Palynology* 145, 275-288
778
779

780
781
782
783
784
785
786
787
788
789
790
791
792
793
794
795
796
797
798
799
800
801
802
803
804
805
806
807
808
809
810
811
812
813
814
815
816
817
818
819
820
821
822
823

Figure Legends

Fig. 1. Map of Lake Baikal and its immediate catchment, showing the location of key sites: Lake Khall, Ol'khon region, Lake Kotokel and Primorsky Mountain Range.

Fig. 2. Age-depth model based on ^{137}Cs and calibrated radiocarbon AMS dates, constructed using 'Bacon' (Blaauw and Christen, 2011). Grey-shaded area represents 95% confidence intervals of modelled ages (black line).

Fig. 3. Pollen, spore and *Pediastrum* coenobia colony relative abundances plotted on the calibrated age scale. Taiga biome scores are also shown – see section 3.2 for details. Significant PCA axis 1 sample scores (+ eigenvalue; EV) and significant compositional turnover (beta diversity; SD units) value for vegetation data is also given ($p = 0.05$; $n=499$). Pollen zones have been delimited using optimal partitioning.

Fig. 4. Total ostracod concentrations (valves/g) are plotted on the calibrated age scale, along with the two most abundant genera *Lymnocythere* sp. and *Candona* sp. The concentration of blackened valves is also given.

Fig. 5. Low-frequency magnetic susceptibility measurements and particle size statistics produced from Folk and Ward (1957) method (mean particle size, sorting, skewness and kurtosis). Sedimentary mean values are shown with a vertical line for each of mean particle size, sorting, skewness and kurtosis.

Fig. 6. PCA biplot of geochemical data. Axis 1 is plotted against axis 2. Axis 1 accounts for significant 73.8% variation in element data. Axis 2 accounts for only 10.0% variation in the data which broken stick shows is not significant.

Fig. 7. Geochemical stratigraphy of Lake Khall. Selected major elements are shown, expressed either as percentages (Al, Ti, K, Si, P, S, Mn, Fe) or concentrations ($\mu\text{g/g}$: Rb, Pb, Ca, Sr). Significant PCA axis 1 sample scores (+ eigenvalue; EV) are also shown.

Fig. 8. Composite stratigraphical plot showing: (i) pollen DCCA axis 1 sample scores; (ii) mean grain size; (iii) pollen-inferred reconstruction anomalies (total annual precipitation – Pann; mean temperature of the coldest month – Tc; mean temperature of the warmest month – Tw); (iv) geochemical ratio of selected elements Sr/Ca ($\times 1000$), Ca/Al, P/Al, Ti/K, K/Rb; (v) concentrations of *Candona* sp.; (vi) oxygen isotope data from Lake Baikal biogenic silica (Mackay et al., 2011); (vii) oxygen isotope data from Dongge Cave, southern China (Wang et al., 2005); (viii) palaeo-temperatures inferred from the GRIP borehole ($^{\circ}\text{C}$) (Dahl-Jensen et al., 1998); (ix) July insolation at 60°N (W/m^2) (Berger and Loutre, 1991)

Figure 1

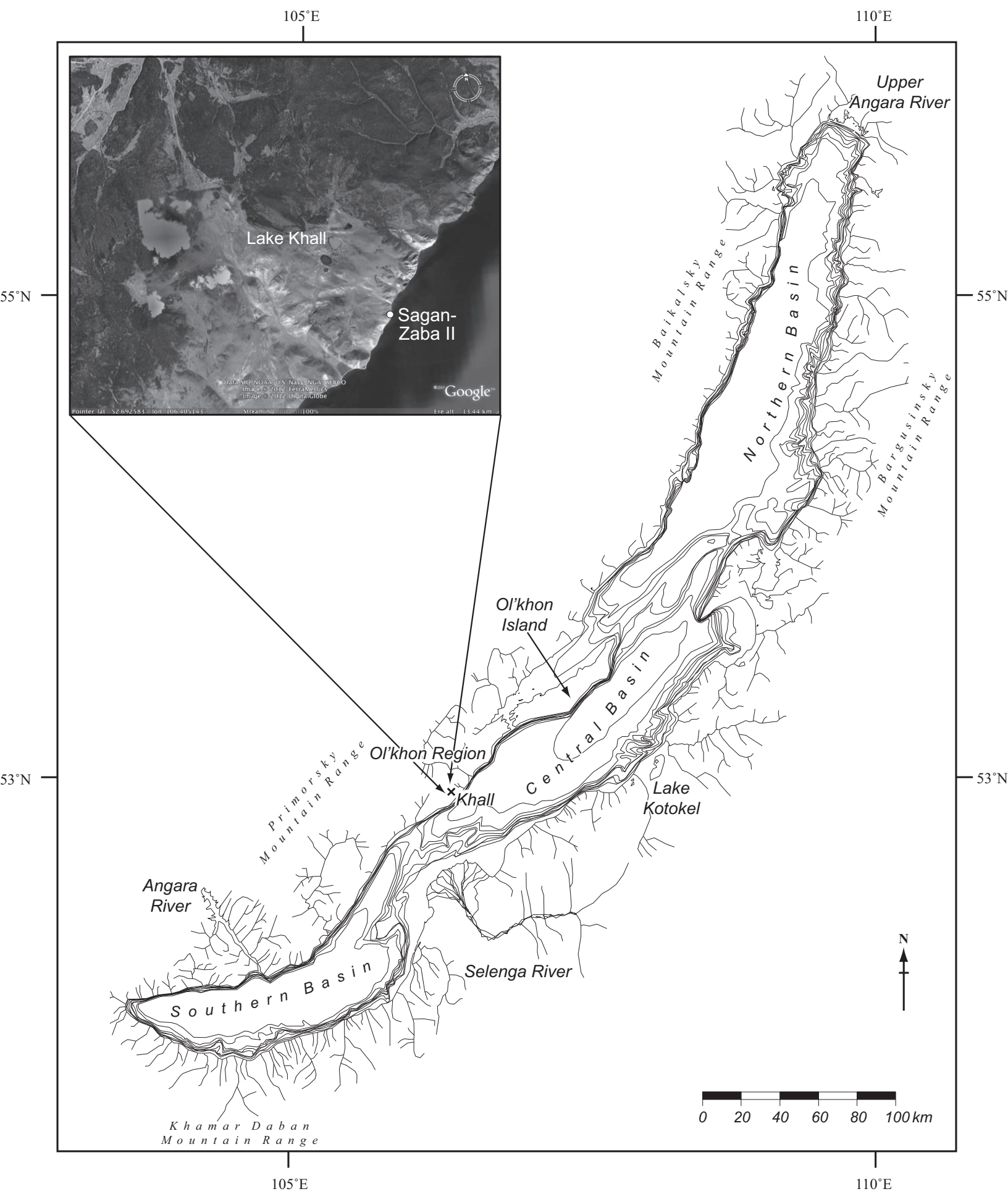


Figure 2

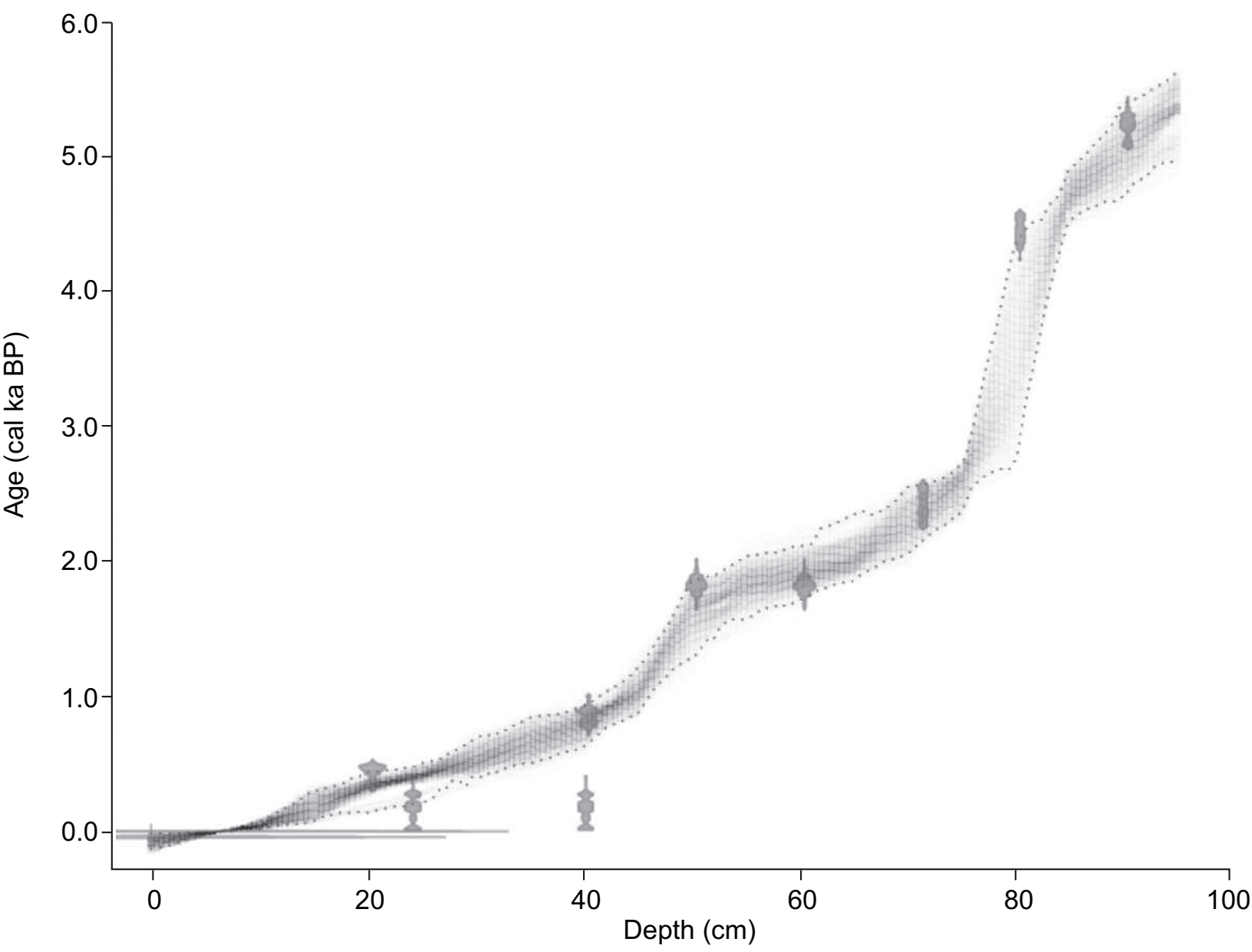


Figure 3

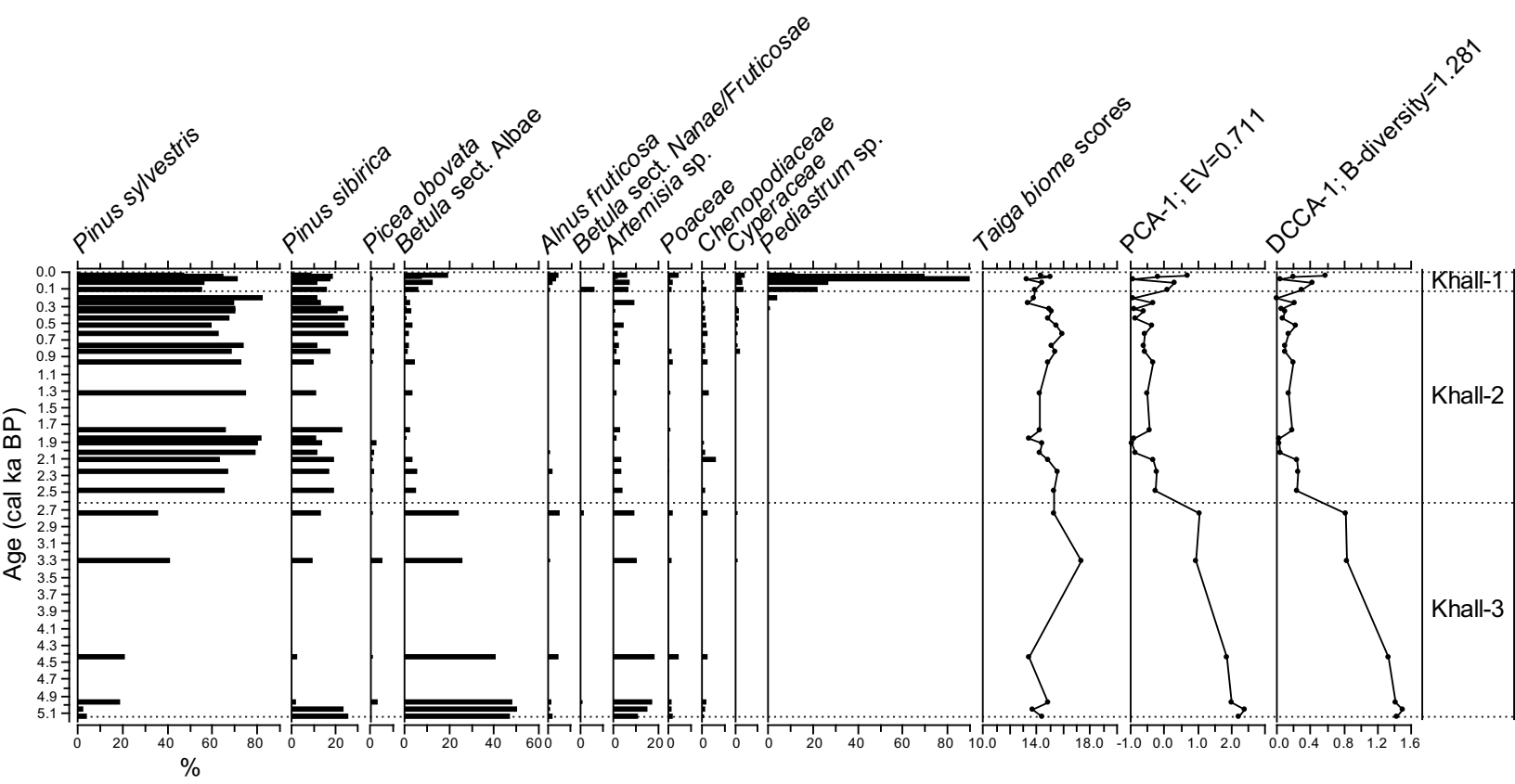


Figure 4

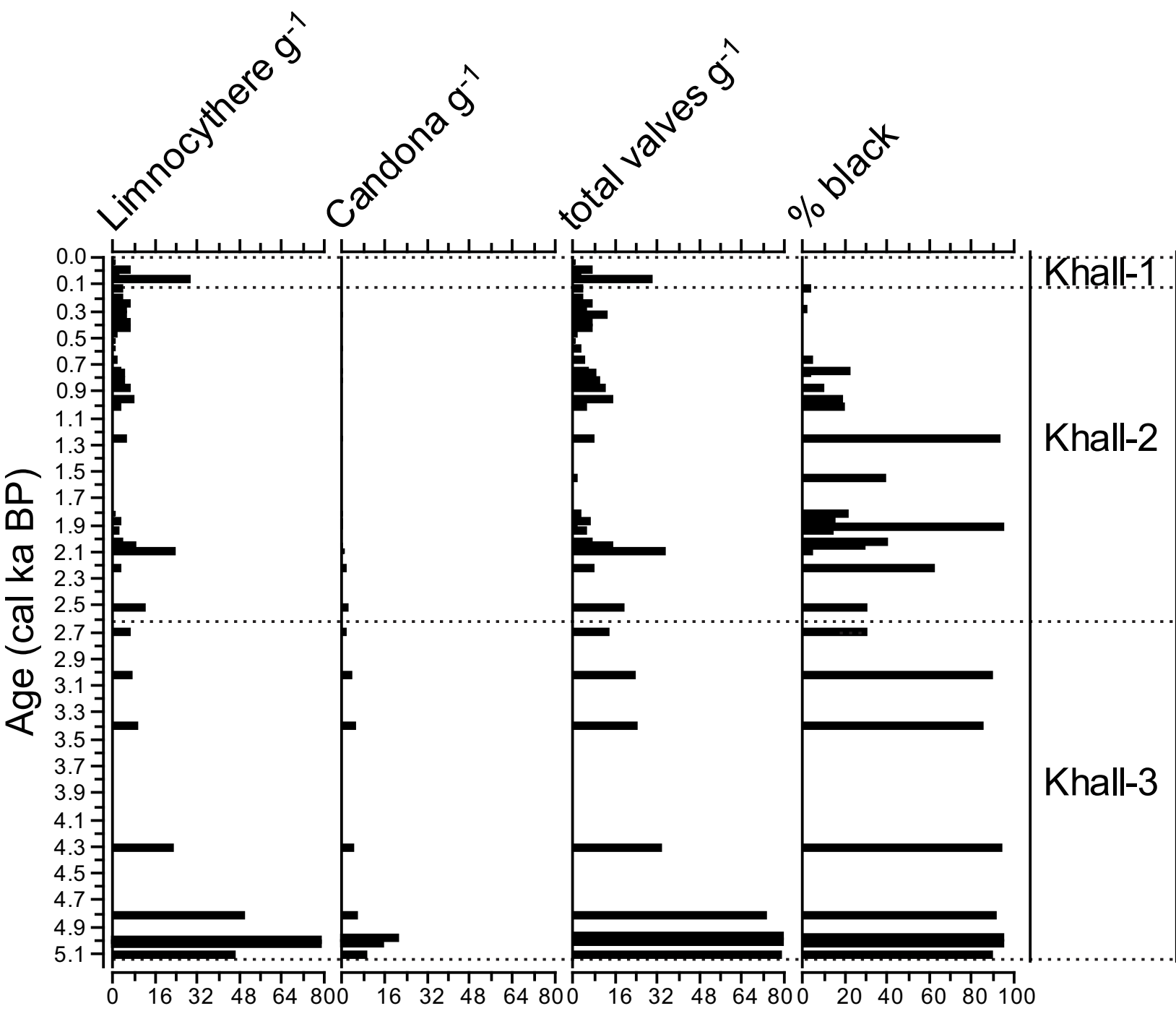


Figure 5

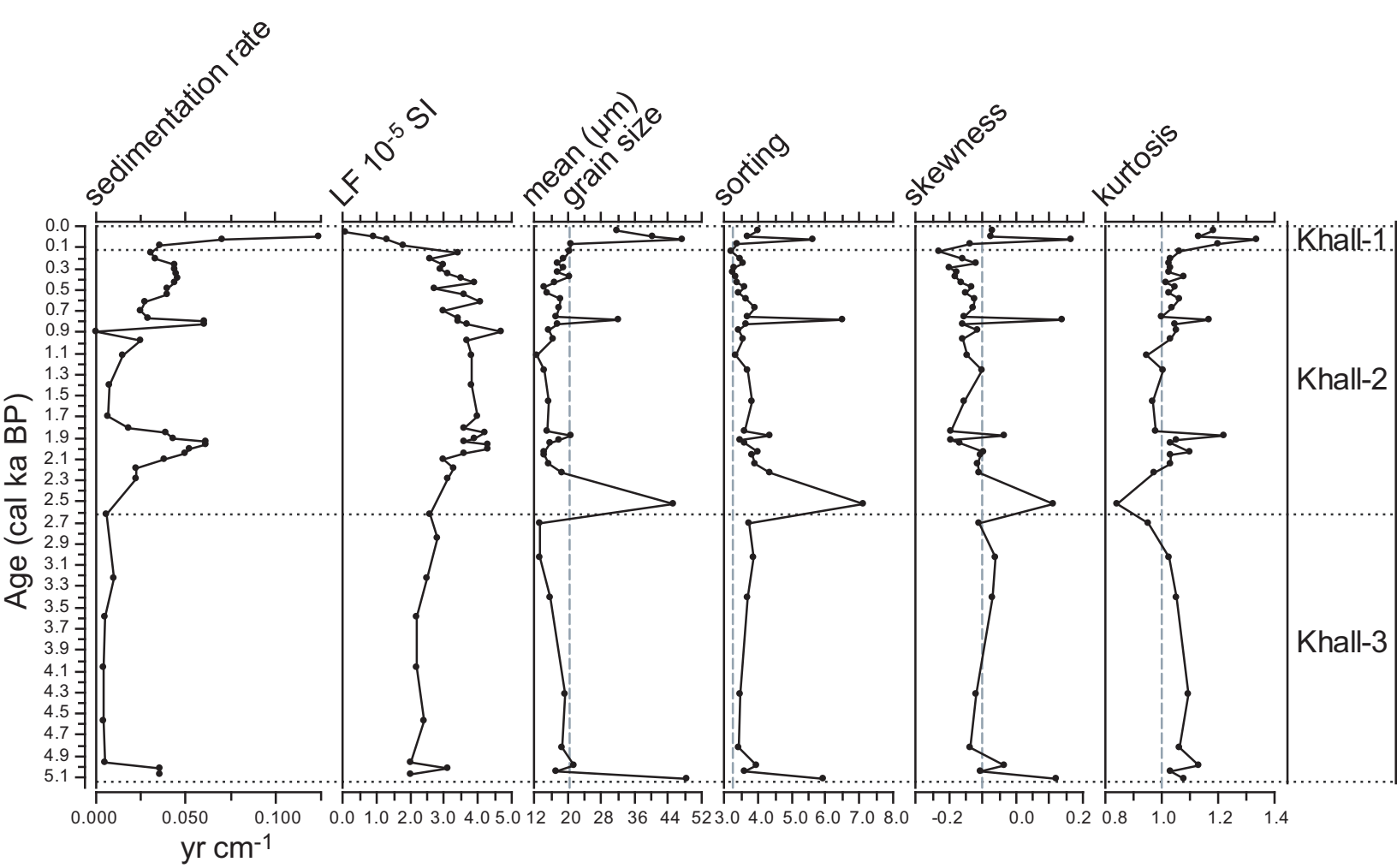


Figure 6

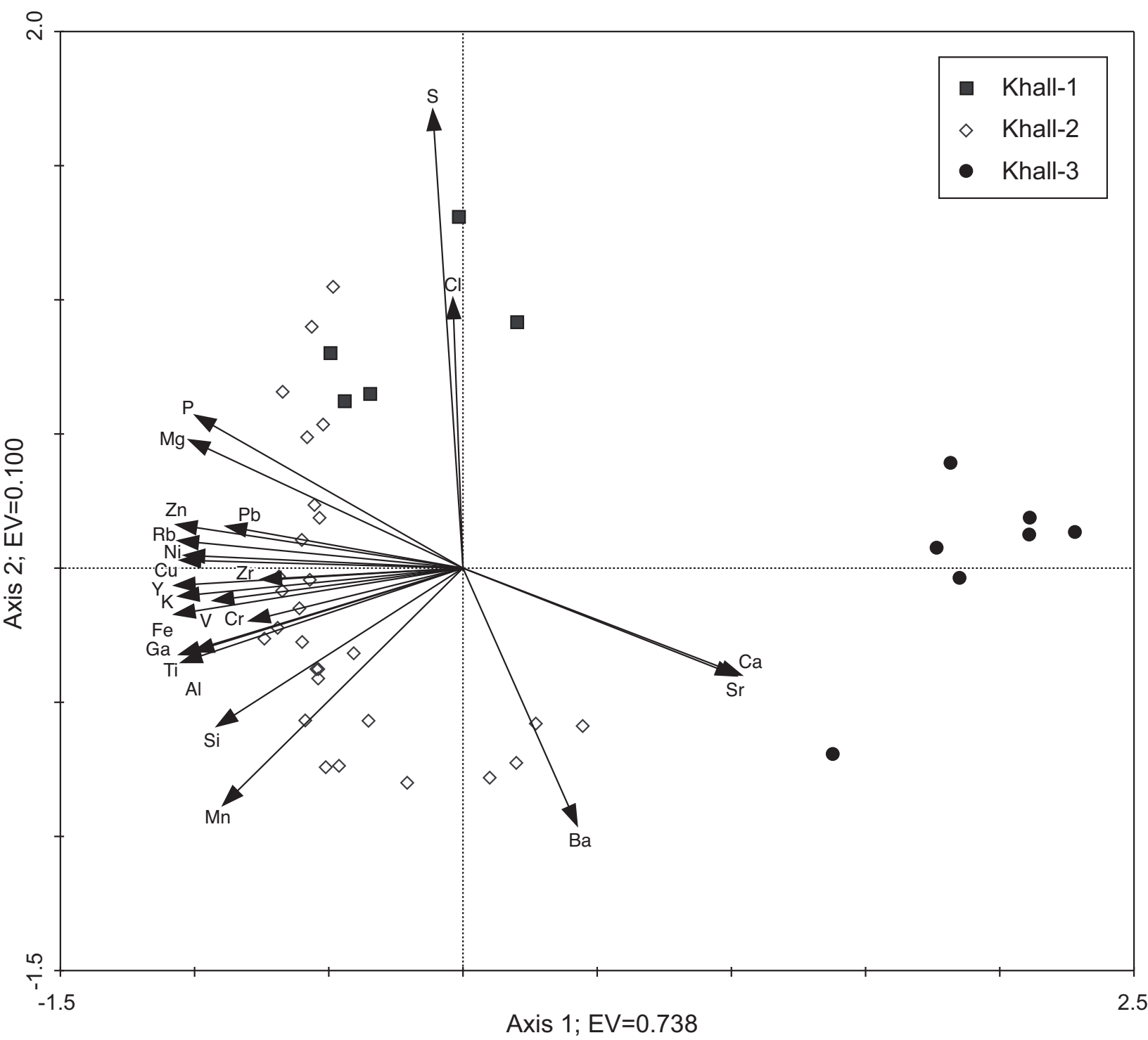


Figure 7

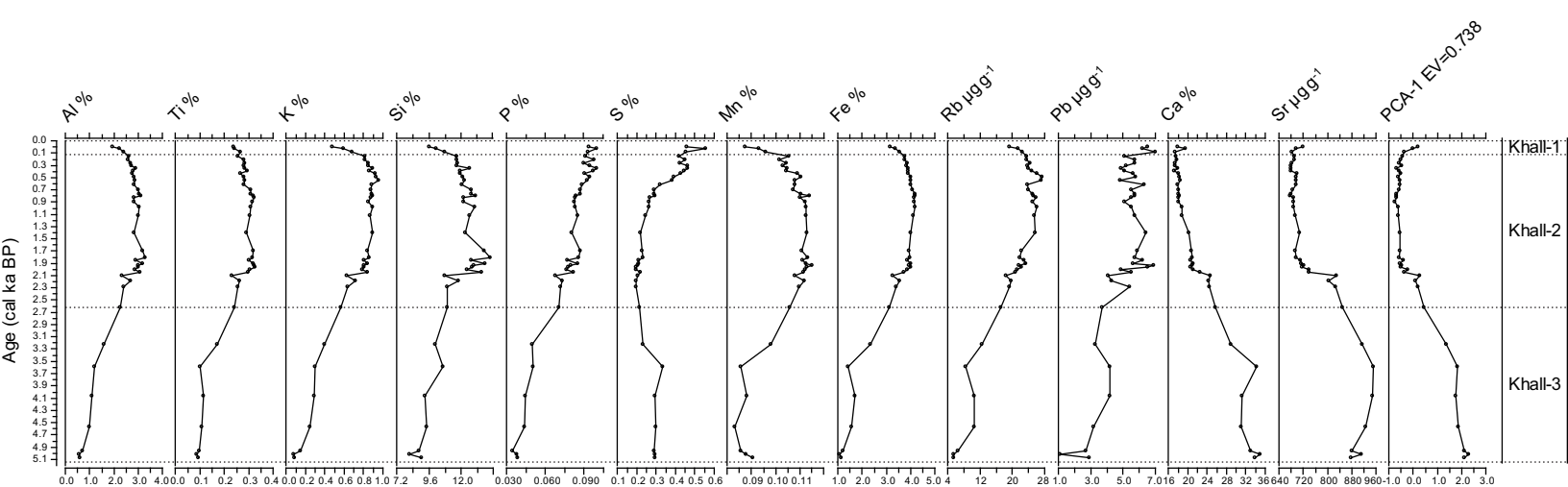


Figure 8

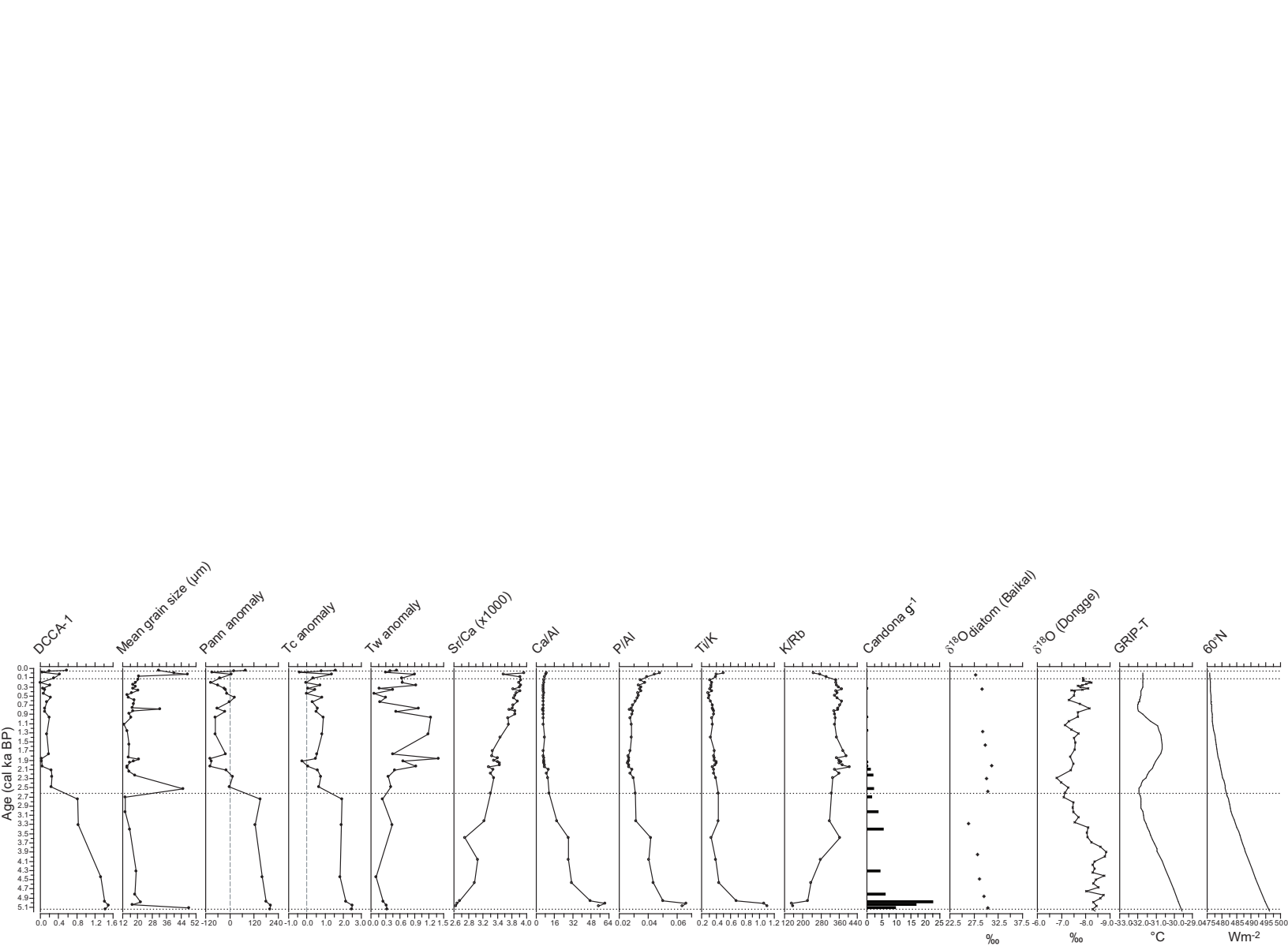


Table 1: Results of AMS radiocarbon dating for Lake Khall sediment core. Depth range and mid-depth are the original depths of samples from core. Calibration of independent ^{14}C dates from the core was performed using IntCal09 radiocarbon calibration curve (Reimer et al., 2009) and OxCal software ver. 4.1.7 (Bronk Ramsey, 2009), assuming the reservoir correction of 150 ± 50 years.

Sample code	Sample material	Depth range, cm	Mid-depth, cm	^{14}C age BP	Calibrated age range calBP (68.2%)		Calibrated age range calBP (95.4%)	
Poz-25686	Contemporary macrophytes	n/a	n/a	105.58±0.33 pMC	n/a	n/a	n/a	n/a
Poz-30449	TOC	20-21	20.5	555±30	626	532	640	519
Poz-25740	<i>Potamogeton</i> seed	24-24.5	24.25	345±30	465	319	485	313
Poz-25682	<i>Potamogeton</i> seed	40-40.5	40.25	330±30	455	316	474	308
Poz-30448	TOC	40-41	40.5	1140±30	1072	980	1169	968
Poz-33695	TOC	50-51	50.5	2110±35	2131	2009	2295	1992
Poz-30447	TOC	60-61	60.5	2105±30	2123	2010	2150	1995
Poz-33696	TOC	71-72	71.5	2605±35	2759	2724	2787	2545
Poz-25683	<i>Potamogeton</i> seed	80-81	80.5	4285±35	4865	4835	4964	4822
Poz-25684	<i>Potamogeton</i> seed	90-91B	90.5	4930±70	5730	5596	5892	5487